

Theoretical model for the hcp-bcc transition in Mg

Renata M. Wentzcovitch and Marvin L. Cohen

Department of Physics, University of California, Berkeley, California 94720

and Materials and Chemical Sciences Division, Lawrence Berkeley Laboratory, Berkeley, California 94720

(Received 18 September 1987)

Using a first-principles total-energy pseudopotential method, we investigate the transition mechanism for a pressure-induced martensitic transformation hcp \rightarrow bcc which occurs in Mg at pressures around 50 GPa. Two internal structural degrees of freedom are selected and one lattice is transformed into the other by relaxing these two parameters continuously. One of the parameters characterizes the relative displacement of the hexagonal layers and corresponds to a transverse phonon at the Brillouin-zone edge A in the hexagonal structure. The other characterizes the distortion of the internal hexagonal angles and corresponds to uniform strain along one of the $[0010]_{\text{hcp}}$ directions. The interaction between these two distortion modes causes important anharmonic effects in the zone-edge phonon and provides a low-energy path for the structural transition. The small activation barrier at the transition indicates that quantum fluctuations between the two structures could be taking place.

I. INTRODUCTION

A large number of metals exist in close-packed phases and under pressure or heat they transform into another close-packed phase. These are called martensitic transformations¹ and for more than 60 years they have been subjected to thorough investigation.

The relationship between the transformed and the original phases is identified by means of x-ray diffraction techniques which show that in several cases there exist definite crystallographic relations between the orientations of the newly formed and the parent crystals. These relations suggest that the process of transformation can, in general, be described by homogeneous deformations of the initial lattice by contractions or dilations or shears parallel to certain planes and directions. Typical examples of these transformations are the tetragonal distortion which relates the bcc and the fcc structures, known as the Bain strain, or the homogeneous shear of every pair of hexagonal planes along the $[\bar{1}100]_{\text{hcp}}$ directions which transforms the hcp structure with $ABAB\dots$ stacking into the fcc phase with $ABCABC\dots$ stacking along the $[111]_{\text{fcc}}$ direction.

Less known, however, is the relationship between the hcp and the bcc phases which was first analyzed by Burgers in Zr (Ref. 2). This metal exhibits a temperature-induced bcc \rightarrow hcp transition in which the hexagonal crystal is formed with its $(0001)_{\text{hcp}}$ basal planes parallel to the $(110)_{\text{bcc}}$ planes of the cubic crystal, with one of the directions $[0010]_{\text{hcp}}$ parallel to one of the $[001]_{\text{bcc}}$ directions. This relationship between orientations suggested a possible transition mechanism which can be described by two strains: a uniform contraction along the $[001]_{\text{bcc}}$ direction and an internal shear of the $(110)_{\text{bcc}}$ planes along the $[1\bar{1}0]_{\text{bcc}}$ directions displacing every second layer to the hcp position.

Although the relationship between the crystallographic directions of these two phases is suggestive, the mechanism

that drives the transition is not easily identified. An early theory³ suggested that the internal shear of the $(110)_{\text{bcc}}$ planes could be caused by a softening of the corresponding phonon mode. The lack of evidence for this softening later led to the suggestion that the transition to the high temperature stable bcc phase in many metals was driven by an excess of entropy in the bcc phase⁴ which had a phonon spectrum on the average lower in energy than the hcp phase. From the point of view of electronic structure, the high-pressure bcc phase has a preference for electrons in the d states⁵ since they participate more actively in forming bonds when nearest-neighbor distances decrease.

More recently the temperature-induced bcc \rightarrow hcp transition was studied by assuming a free energy Landau expansion in terms of these two strain components and mapping the problem into a two-dimensional magnetic analog with the martensitic transition symmetry.⁶ The model was then investigated by using Monte Carlo simulation and the results suggested that the transition could be caused by strong anharmonicities. Although the model was simple, it motivated a total energy calculation of such a transition in Zr (Ref. 7) in which the temperature dependence of the phonon frequencies was treated using a perturbative formalism.

An ideal way to study the mechanism of the martensitic transformation is to investigate directly the shape of the free energy surfaces with respect to the thermodynamical variables including all internal structural degrees of freedom. At zero temperatures within the static lattice approximation this can be achieved by using the first-principles total energy techniques to compute the structural energies of the pressure-induced martensitic transition.

In this paper we investigate such energy surfaces at zero temperature in Mg, where a typical martensitic transformation hcp \rightarrow bcc occurs for pressures around 50 GPa. This is done by using the pseudopotential method

within the local-density-functional formalism which has been successful in studying various structural properties of metals, semiconductors, and interfaces. This paper is organized in the following way: Sec. II contains a description of the hcp \rightarrow bcc transition in terms of the minimum structural degrees of freedom, which are the parameters necessary to determine the energy path for the transition. In Sec. III we give a brief account of the calculational procedure together with the main results of the hcp \rightarrow bcc transition. The conclusions are presented in Sec. IV.

II. DESCRIPTION OF THE TRANSITION

To understand the bcc \rightarrow hcp phase transition and the correct variables that describe it, it is helpful to examine the two structures from the following perspective: Fig. 1(a) shows the bcc structure in which some of the (110) planes have their distorted hexagons drawn with heavier lines. These hexagons have two central angles $\theta = 70.53^\circ$ and four others equal to 54.77° . The stacking of these planes along the [110] direction is according to the *ABAB...* sequence, which is similar to the stacking of the hexagonal layers in the hcp structure. Each atom, for instance in the *A* layers, lies on top of (below) a "bond" between two second-nearest-neighbor atoms in the *B* layers (on "bridge" sites). In the hcp phase the atoms lie on top of centers of triangles formed by three equidistant atoms (on "hollow" sites). Therefore, the minimum energy path from the bcc to the hcp phase may result from a simultaneous distortion of the angle θ , i.e., strain along

$[001]_{\text{bcc}}$ direction, and a displacement of the atoms in the *B* layers from the bridge to the hollow sites [see Fig. 1(c)]. From this perspective it appears that the values of these two variables should be strongly correlated and as the atoms of the *B* layers move from the bridge sites towards the hollow sites, the second-nearest-neighbor atoms forming the bridges in the *A* layers are allowed to come closer. This reduces the angle θ approaching 60° and eventually becoming first neighbors in the hcp structure. Figure 1(b) shows the hcp structure with an embedded body centered cube distorted according to the above recipe.

Consider now the c/a ratio in the hcp structure which results from this combination of shear and strain. Since the distance between the (110) planes in the bcc structure does not change by simply changing θ and x , the final c/a ratio is equal to the ideal $\sqrt{8/3}$. To see this consider the bcc and hcp phases as particular cases of a general triclinic structure which has two basis vectors oriented as indicated in Fig. 1(c), and the third one perpendicular to these two vectors. In the bcc phase c corresponds to twice the distance between the neighboring $(110)_{\text{bcc}}$ planes, i.e., $\sqrt{2}b$ where b is the lattice constant, while a is equal to $(\sqrt{3}/2)b$. This relation suggests that in an ideal hcp \rightarrow bcc transition, the c/a ratio, which is a possible degree of freedom, should be approximately constant.⁸ In this study most of the results were obtained without relaxing this parameter since its largest departure from the ideal value occurs in the hcp structure where $c/a \approx 1.623$ and the changes in the total energies obtained by relaxing it are insignificant compared to the energies involved in the relaxation of the degrees of freedom x and θ .

III. CALCULATIONS AND RESULTS

A. General aspects

The present calculation uses the pseudopotential total energy method⁹ within the local density approximation (LDA) (Ref. 10) to calculate the total energies per atom of the solid in different structures. We used a plane-wave expansion corresponding to energies up to 12 Ry and chose 112k points in the irreducible Brillouin zone (BZ) of the common triclinic structure, which corresponds to 48k points in the BZ of the hcp structure. To describe the exchange correlation potential we used the Wigner interpolation formula.¹¹ The pseudopotential was generated from the same atomic configuration used in a previous calculation;¹² however, a core correction is added to the exchange correlation potential.¹³ This leads to a more repulsive pseudopotential with respect to the previous calculation and slightly increases the values of lattice constants and bulk modulus. Our results are summarized in Table I while the total energy curves, which are fit to the Murnaghan equation,¹⁴ are displayed in Fig. 2. Within the range of volumes and pressures studied the calculated and measured c/a ratios are shown to be approximately constant.¹⁵

Figure 2 illustrates the nature of the structural transition we are studying. Because the two structures have similar structural energies along a considerable range of

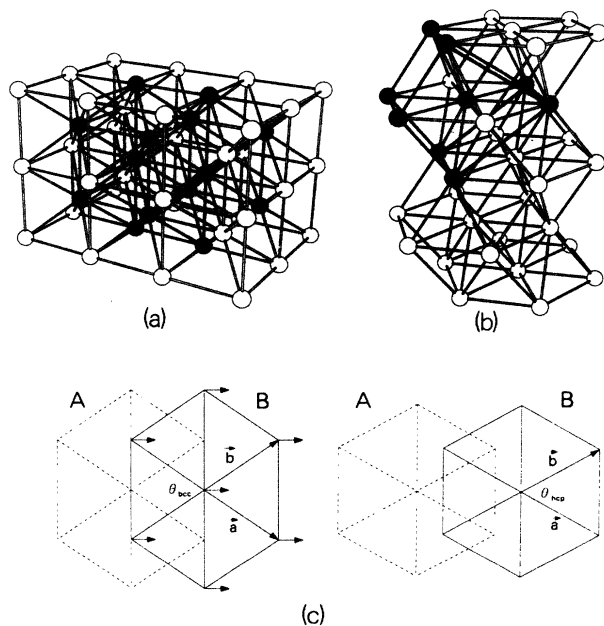


FIG. 1. Structural relationship between the hcp and the bcc phases. (a) The distorted hexagons in the (110) planes of the bcc structure. (b) Distorted body-centered cube imbedded in the hcp structure. (c) Transformation of the $(110)_{\text{bcc}}$ plane into $(0001)_{\text{hcp}}$ plane where the atomic movements are indicated by arrows.

TABLE I. Comparison of the calculated structural properties of Mg with experiment and other calculations.

	hcp	bcc	hcp→bcc transition	
B_0 (GPa)	3.7 ^a	3.5 ^a	P_T (GPa)	60 ^a
	3.5 ^b			50 ^e
	3.54 ^c			57 ^e
a (Å)	3.18 ^a	3.54 ^a	$\frac{V_T}{V_0}$	50±6 ^f
	3.16 ^b			0.57 ^a
	3.21 ^d			0.58 ^e
c (Å)	5.16 ^a		$\frac{\Delta V}{V_0}$	0.56 ^e
	5.09 ^b			0.59±0.2 ^f
	5.21 ^d			≤1% ^a
$\frac{c}{a}$	1.623 ^a			≈1% ^f
	1.61 ^b			
	1.623 ^d			
Cohesion (eV/pair)	1.62 ^a	1.54 ^a		
	1.64 ^b			
	1.51 ^d			

^aThis work (without zero-point motion corrections).

^bPseudopotential calculation (Ref. 12).

^cExperiment (Ref. 16).

^dExperiment (Ref. 17).

^eGPT and LMTO (Ref. 5).

^fExperiment (Ref. 15).

volumes around the transition, there is a small change of volume involved in the transition. A small relative shift of energies between the two phases can generate a relatively large uncertainty in the transition pressure P_T or transition volume V_T .

Table I shows that the calculated transition pressure is a little larger than the experimental value while the transition volume is slightly smaller. This suggests that the bcc total energy curve should be shifted by a small amount toward the hcp curve to give agreement with experiment. This shift could be caused by the difference in zero-point motion energies E_{ZP} between the two structures. This difference can be estimated by using the Debye model in which $E_{ZP} = \frac{3}{4}k_B\Theta_D$, where Θ_D is the Debye temperature. In the hcp phase this correction is 6 mRy/pair ($\Theta_D^{\text{hcp}} = 400$). Although for the bcc phase the Debye temperature Θ_D^{bcc} is not known, we follow Friedel⁴ and assume that the overall phonon spectrum in this phase has lower energies, which are expected to scale with the number of neighbors, i.e., 8 for bcc and 12 for fcc and hcp, and hence the Θ_D^{bcc} should also scale with the same factor. We conclude that $(E_{ZP}^{\text{hcp}} - E_{ZP}^{\text{bcc}}) \approx 2$ mRy/pair at zero pressure and that a relative shift of the two curves by this amount would bring our result for the transition pressure in good agreement with experiment. This argument has already been shown to be important to

explain the temperature-induced phase transitions in Be.¹⁸ At zero pressure and temperature the energy ordering of Be phases is (hcp, fcc, bcc), but it transforms into the bcc at 1530 K. In this case the lower phonon spectrum of the bcc structure is responsible for an excess of entropy in the bcc phase with respect to the other 12-fold coordinated structures, and at high temperatures the Gibbs free energy favors this phase.

B. The transition

The transition is studied by selecting the variables V , x , and θ , which specify, respectively, volume, internal shear of hexagonal layers, and internal hexagonal angle. The shear corresponds to a transverse phonon at the zone edge A in the hcp phase or N in the bcc phase. The angle θ corresponds to strain along the $[001]_{\text{hcp}}$ or $[001]_{\text{bcc}}$ directions. To convert the variable V into nearest-neighbor distances a_n recall that $a_n^{\text{bcc}} = 0.866V^{1/3}$ and $a_n^{\text{hcp}} = 0.891V^{1/3}$.

Figure 3 shows the total energy curves of the distorted structures as a function of the variable x . Each dashed curve corresponds to a different angle θ as specified, while volume is kept fixed and equal to $0.6V_0$, where V_0 is the equilibrium volume of the hcp structure. The value $x = 0$ corresponds to the hcp structure, while $x = 1$ corresponds to bcc. This figure displays strong correlation be-

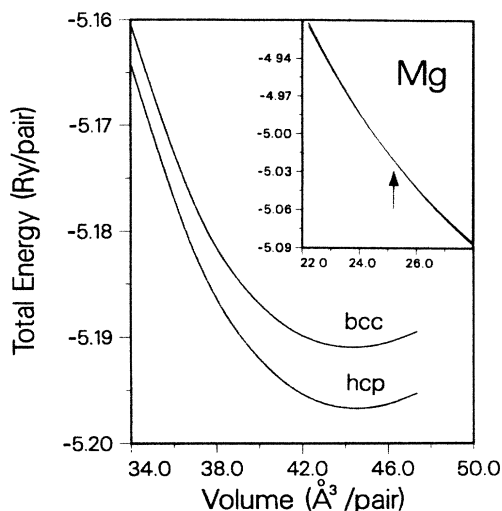


FIG. 2. Total energy curves of the hcp and bcc structures as a function of the primitive cell volume. The inset shows the similarity of energies between the structures around the transition which is indicated by the arrow.

tween the two variables and for each angle, the layers displace with respect to each other to minimize the energy. This correlation between variables results in an opening of the bonds forming the bridges in the A layers as the atoms in the B layers move from the hollow to the bridge sites.

The lower solid line corresponds to the energy barrier between the two structures and is obtained by minimizing the energy $U(x, \theta, 0.6V_0)$ with respect to θ at specific x 's. The observed correlation between these variables causes strong anharmonic effects in the zone-edge phonon under consideration and provides a low-energy path for the transition. It can be seen that at this volume the barrier height is approximately 3 mRy/pair, which is smaller

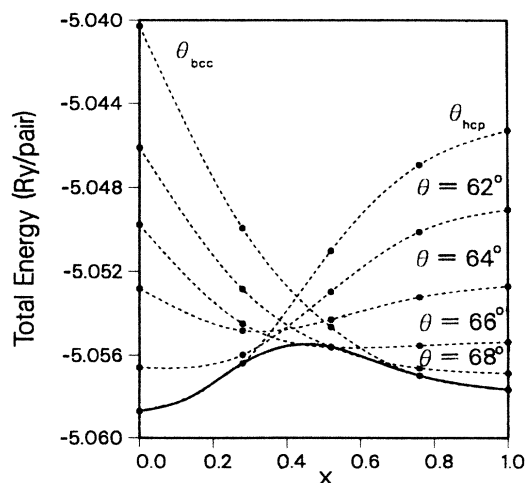


FIG. 3. Calculated total energies as function of the two parameters x and θ which describe the lattice deformation: $\theta_{\text{hcp}} = 60^\circ$, $x_{\text{hcp}} = 0.0$, $\theta_{\text{bcc}} = 70.53^\circ$, $x_{\text{bcc}} = 1.0$. The volume is fixed and equal to $0.6V_0$, where V_0 is the equilibrium volume.

than the zero-point motion energy of both structures (at this volume $E_{\text{ZP}}^{\text{hcp}} \approx 7.0$ mRy and $E_{\text{ZP}}^{\text{bcc}} \approx 4.7$ mRy in the Debye approximation). Hence at this volume both structures seem to be accessible in terms of energy, and quantum fluctuations could take place between them.

In Fig. 4 the c/a ratio which minimizes the energy at $V = 0.6V_0$ is displayed. The points were obtained by maintaining the parameter θ constant and equal to that which minimizes the energy at the ideal c/a ratio at the respective value x . As expected (see Sec. II), this ratio approaches the ideal value 1.633 when the layers move toward the bcc position and x approaches 1.0. The relaxation of this degree of freedom decreases the energy by less than 0.1 mRy/pair with respect to the ideal ratio. This value is much smaller than the energy gained in the relaxation of the parameters x and θ , therefore it is kept equal to 1.633 in the rest of this study.

Figure 5(a) displays the shape of the barriers at three different volumes around the transition, while Fig. 5(b) shows the dependence of the angle θ on the displacement parameter x . These energy barriers correspond to the upper-bound limit since relaxation of other degrees of freedom, beside x and θ , could decrease them slightly. They also reveal the overall lower phonon spectrum of the bcc phase. As pointed out before, the zero-point motion energies E_{ZP} , at the equilibrium positions, are larger than the barriers heights; therefore, there is a considerable chance that the barriers are frequently tunneled and the transition to happen back and forth. Although we do not include E_{ZP} in the computed free energies, we keep it in mind because it imposes a limit on the predictions a static theory can make. The present study indicates that the considered transition pushes the static approximation to its limit and there is a large uncertainty in the particles position. This behavior, together with nonhydrostatic stresses, could be causing the pressure range of coexistence between the two structures, a situation which is not particular for Mg but is a common aspect of many reports on pressure- or temperature-induced martensitic transformations.

The similarities between the internal energies of the two phases in a wide range of volumes around the transition indicate that pressure, which is the driving mechanism of the transition, and volume are interchangeable

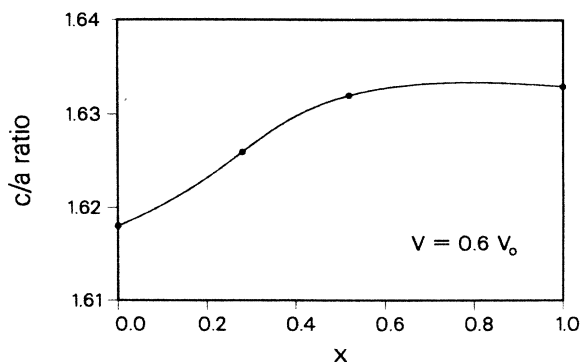


FIG. 4. Calculated c/a ratio as function of the parameter x (see text).

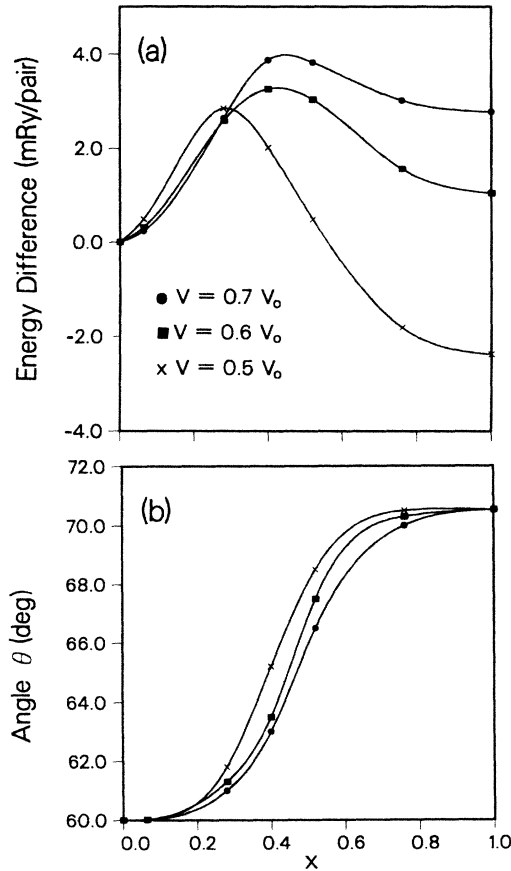


FIG. 5. (a) Minimized energy differences as a function of the parameter x indicating the relative stabilities and the energy barriers between the hcp and the bcc phases around the transition; these volumes correspond to the following pressures: ●, 43 GPa; ■, 60 GPa; ×, 80 GPa. (b) Dependence of the angle θ on the parameter x for the three considered pressures.

thermodynamical variables within this range. Therefore, a direct calculation of the difference between the internal energies $U(V', \xi; S=0)$ of the two phases corresponds approximately to the difference in the Gibbs free energy $G(P', \xi; T=0)$. In these expressions ξ represents internal structural degrees of freedom, $S=0$ is the entropy at $T=0$ and

$$P' = \left. \frac{\partial U}{\partial V} \right|_{\xi = \text{cte}} \Big|_{V=V'}$$

(Ref. 19). This means that the energy barriers plotted in Fig. 5(a) correspond to the Gibbs free energy at the following pressures: ●, 43 GPa; ■, 60 GPa; ×, 80 GPa. From this perspective it can be seen as a typical first-order phase transition in which pressure is the driving force and x is the order parameter. If desired, a free energy expansion in powers of x could be attempted, similarly to the Landau expansions which describe temperature-induced transitions. These expansions can be successful

provided the coupling of the variables x and θ , as indicated in Fig. 3, are appropriately incorporated.

The above point is worth considering in detail because similar expansions can be tried for other pressure-induced martensitic transformations whenever equivalent variables x and θ can be identified. For example, the fcc \rightarrow hcp transition, typical of Co and Co alloys, can be described by a successive displacement of every two adjoining $(111)_{\text{fcc}}$ planes toward the $[11\bar{2}]_{\text{fcc}}$ direction. Such a displacement transforms the $(111)_{\text{fcc}}$ plane with $ABCABC\dots$ stacking into $(0001)_{\text{hcp}}$ planes with $ABAB\dots$ stacking. Even though the two structures are formed by perfect hexagonal layers with all internal angles equal to 60° , the angle whose bisector corresponds to the direction of displacement must also deform during the relative movement of layers, since bridges of second-nearest-neighbor bonds are crossed during this movement. The fcc \rightarrow bcc transition can also be described by relative displacement of layers in which $(111)_{\text{fcc}}$, with $ABCABC\dots$ stacking, transforms into $(110)_{\text{bcc}}$, with $ABAB\dots$ stacking of distorted hexagonal layers. This mechanism proposed by Nishiyama¹ is different from the Bain tetragonal distortion typical of carbon steels and usually invoked to explain the fcc \rightarrow bcc transition. A proper account of the correlation between the variables x and θ can be fundamental in determining the lowest energy path between the two structures and therefore the mechanism of transition.

IV. CONCLUSIONS

We have performed a first-principles total-energy study of a pressure-induced hcp \rightarrow bcc martensitic transformation in Mg. This is done by selecting two internal structural degrees of freedom and distorting one lattice into the other by changing these two parameters continuously. One of them characterizes the relative displacement of the hexagonal layers and corresponds to a transverse phonon at the zone edge A in the hcp phase or at N in the bcc phase. The other characterizes the distortion of the internal hexagonal angles and corresponds to strain along the $[0010]_{\text{hcp}}$ or $[001]_{\text{bcc}}$ directions. A strong correlation between these two parameters is observed. This causes important anharmonic effects in these zone edge phonons during the transformation and provides a low-energy path for the structural transition. This correlation between the two structural parameters is possibly a typical feature of the other martensitic transitions between closed packed structures, since similar displacements of layers are involved in most cases.

A close inspection of the free energy surfaces reveals that at the transition the activation barrier involved is smaller than the zero-point motion energies of the two structures. This suggests that, at this point, quantum fluctuations between the two structures could be taking place.

ACKNOWLEDGMENTS

One of us (R.M.W.) is pleased to acknowledge financial support from the Conselho Nacional de Desenvolvimento Científico e Tecnológico (CNPq) of Brazil. We thank M.

Y. Chou for providing the IBM computer codes, P. K. Lam for many discussions, A. G. Kachaturyan for a seminal discussion, H. Olijnyk for a detailed account of his experimental data, R. Jeanlouz for his interest, and W. Basset for providing us with data on iron. This work was supported by the National Science Foundation Grant

No. DMR8319024, and by the Director, Office of Energy Research, Office of Basic Energy Sciences, Material Science Division of the U.S. Department of Energy under Contract No. DE-AC03-76SF00098. Cray computer time was provided by the Office of the Energy Research of the Department of Energy.

¹Z. Nishiyama, *Martensitic Transformations* (Academic, New York, 1978).

²W. G. Burguers, *Physica* **1**, 561 (1935).

³C. Zener, *Phys. Rev.* **71**, 846 (1958).

⁴J. Friedel, *J. Phys. (Paris) Lett.* **35**, L59 (1974); **43**, 985 (1982).

⁵M. Moriarty and A. K. McMahan, *Phys. Rev. Lett.* **48**, 809 (1972).

⁶P.-A. Lindgard and O. G. Mouritsen, *Phys. Rev. Lett.* **57**, 2458 (1986).

⁷Y.-Y. Ye, Y. Chen, K.-M. Ho, B. N. Harmon, and P.-A. Lindgard, *Phys. Rev. Lett.* **58**, 1769 (1987).

⁸W. Basset and E. Huang (unpublished). This investigation of the pressure-induced bcc→hcp transition in iron indicates that in this metal there is an anomalous departure of the c/a ratio from the ideal one during the coexistence of the two phases. The origin of the deviation is analyzed and several causes are suggested.

⁹M. L. Cohen, *Phys. Scr. T* **1**, 5 (1982).

¹⁰*Theory of Inhomogeneous Electron Gas*, edited by S. Lundqvist and N. H. March (Plenum, New York, 1983).

¹¹E. Wigner, *Phys. Rev.* **46**, 1002 (1934).

¹²M. Y. Chou and M. L. Cohen, *Solid State Commun.* **57**, 785 (1986).

¹³S. G. Louie, S. Froyen, and M. L. Cohen, *Phys. Rev. B* **26**, 1738 (1982).

¹⁴F. D. Murnaghan, *Proc. Nat. Acad. Sci. U.S.A.* **30**, 244 (1944).

¹⁵H. Olijnyk and W. B. Holzapfel, *Phys. Rev. B* **31**, 4682 (1985).

¹⁶C. Kittel, *Introduction Solid State Physics*, 5th ed. (Wiley, New York, 1976).

¹⁷W. Koster and H. Franz, *Met. Rev.* **6**, 1 (1961).

¹⁸P. K. Lam, M. Y. Chou, and M. L. Cohen, *J. Phys. C* **17**, 2065 (1984).

¹⁹Although the interchangeability of V and P around the transition, as displayed in Fig. 2, is clear only at $\xi_{\text{hcp}}=(x=0.0, \theta=60.00^\circ)$ and $\xi_{\text{bcc}}=(x=1.0, \theta=70.53^\circ)$, it is also true at other intermediary ξ 's. A direct calculation of $U(V, \xi)$, as displayed in Fig. 5, shows that the total energy curves as function of volume for intermediary ξ 's are also parallel to the hcp curve, and the largest departure of parallelism occurs in the bcc phase.